PLOS ONE

RESEARCH ARTICLE

Twitter reveals human mobility dynamics during the COVID-19 pandemic

Xiao Huang[1,2], **Zhenlong Li**[1]*, **Yuqin Jiang**[1], **Xiaoming Li**[3], **Dwayne Porter**[4]

1 Geoinformation and Big Data Research Lab, Department of Geography, University of South Carolina, Columbia, SC, United States of America, **2** Department of Geosciences, University of Arkansas, Fayetteville, AR, United States of America, **3** Department of Health Promotion, Education, and Behavior, Arnold School of Public Health, University of South Carolina, Columbia, SC, United States of America, **4** Department of Environmental Health Sciences, Arnold School of Public Health, University of South Carolina, Columbia, SC, United States of America

* zhenlong@sc.edu

Citation: Huang X, Li Z, Jiang Y, Li X, Porter D (2020) Twitter reveals human mobility dynamics during the COVID-19 pandemic. PLoS ONE 15(11): e0241957. https://doi.org/10.1371/journal.pone.0241957

Editor: Song Gao, University of Wisconsin Madison, UNITED STATES

Received: June 24, 2020

Accepted: October 23, 2020

Published: November 10, 2020

Data Availability Statement: Twitter data was collected using Twitter's public Streaming API from the public domain following Twitter's Developer Agreement. Following Twitter's policy on "Redistribution of Twitter content" (https://developer.twitter.com/en/developer-terms/more-on-restricted-use-cases), the geotagged tweet IDs used in this analysis are made publicly available on Harvard Dataverse (https://doi.org/10.7910/DVN/KRYMOX). The user count for both types of distance calculations in each country and user count for both types of distance calculation in each

Abstract

The current COVID-19 pandemic raises concerns worldwide, leading to serious health, economic, and social challenges. The rapid spread of the virus at a global scale highlights the need for a more harmonized, less privacy-concerning, easily accessible approach to monitoring the human mobility that has proven to be associated with viral transmission. In this study, we analyzed over 580 million tweets worldwide to see how global collaborative efforts in reducing human mobility are reflected from the user-generated information at the global, country, and U.S. state scale. Considering the multifaceted nature of mobility, we propose two types of distance: the single-day distance and the cross-day distance. To quantify the responsiveness in certain geographic regions, we further propose a mobility-based responsive index (MRI) that captures the overall degree of mobility changes within a time window. The results suggest that mobility patterns obtained from Twitter data are amenable to quantitatively reflect the mobility dynamics. Globally, the proposed two distances had greatly deviated from their baselines after March 11, 2020, when WHO declared COVID-19 as a pandemic. The considerably less periodicity after the declaration suggests that the protection measures have obviously affected people's travel routines. The country scale comparisons reveal the discrepancies in responsiveness, evidenced by the contrasting mobility patterns in different epidemic phases. We find that the triggers of mobility changes correspond well with the national announcements of mitigation measures, proving that Twitter-based mobility implies the effectiveness of those measures. In the U.S., the influence of the COVID-19 pandemic on mobility is distinct. However, the impacts vary substantially among states.

1. Introduction

The outbreak of Coronavirus disease (COVID-19) caused by the SARS-CoV-2 virus is a public health emergency that raises concerns worldwide, leading to serious health, economic, and social challenges. As of June 23, 2020, there had been a total of 8,993,659 infections and

state are provided as the Supporting Information: S1 Table.docx and S2 Table.docx.

Funding: The research is supported by National Science Foundation, https://www.nsf.gov/, (2028791) to ZL, XL and DP; and University of South Carolina COVID-19 Internal Funding Initiative, https://sc.edu/about/offices_and_divisions/research, (135400-20-54176) to ZL and XL. The funders had no role in study design, data collection and analysis, decision to publish, or preparation of the manuscript.

Competing interests: The authors have declared that no competing interests exist.

469,587 deaths globally [1], and these figures are progressively increasing every day. On March 11, 2020, the World Health Organization (WHO) reassessed the situation and officially declared COVID-19 as a pandemic, urging countries and regions worldwide to join forces [2]. Since then, major behavioral, clinical, and intervention policies (both strict and loose) have been undertaken to reduce the spread and prevent the persistence of the virus in human populations.

An initial outbreak of COVID-19 was first declared in Wuhan, China in January 2020 [2], before cases were reported in European countries, most notably Italy, France, and the UK. In the United States, the first confirmed case occurred on January 19, 2020, in Snohomish County, Washington. Shortly after, the U.S. has become the new epicenter of the disease as it surpassed Italy in terms of confirmed cases on March 26, 2020 [3]. As of June 23, 2020, there had been a total of 2,268,753 confirmed cases (25.2% of global cases) and 119,761 deaths (25.5% of global deaths) in the U.S. alone [1]. To contain the COVID-19 pandemic, one of the non-pharmacological epidemic control measures is to reduce the transmission rate of SARS--COV-2 in the population via social distancing or other similar (self) quarantine measures [4], with the ultimate goal to reduce person-to-person interactions. Studies have found notable declines in transmission rates after the implementation of mobility-reducing policies in China, Korea, and many European countries [5–8]. Despite the success of these efforts, not all countries/regions chose to handle the pandemic in a similar manner [9, 10]. The discrepancies in policies and measures at different geographical levels urge an approach to monitoring the mobility dynamics in response to the pandemic, as mobility patterns largely indicate how people respond to the pandemic and whether policies are implemented effectively [11–13].

Since the initial outbreak of COVID-19, numerous efforts have been made, by incorporating the emerging concept of "Web 2.0" [14], "Big Data" [15], and "Citizen as Sensors" [16], to obtain timely information regarding whether people are actively reducing their exposure to COVID-19 by reducing distances traveled, and by how much. Companies like Google and Apple have released their aggregated and anonymized community mobility reports based on data collected from their services (i.e., Google Location Services and Apple Maps). Those reports are updated on a daily basis and can be easily downloaded. In addition, authorities started to collaborate with mobile network operators to estimate and visualize the effectiveness of control measures [11, 17], in light of the previous success of mobile phone data in assisting the modeling of the spread of other epidemics [18–20]. Shortly after the outbreak in China, mobility data from Baidu, a famous Chinese online platform, have been put into use to evaluate the effectiveness of the lockdown measure in Wuhan [5]. Leading telecommunication firms also contribute by collaborating with local authorities to estimate the efficiency of travel restrictions as well as to identify the impact of other mobility-reducing related measures [21, 22]. In the U.S., Descarte Lab (www.descarteslabs.com/mobility) has released mobility statistics derived from mobile devices, aiming to facilitate the acquisition of rapid situational awareness at the State- and County-level. City-level studies have also been conducted. For example, locational data from Cuebiq (https://www.cuebiq.com/), gathered via over 180 mobile applications, were used to monitor how social distancing guidelines are implemented on a daily basis in the city of Boston, MA [11]. However, privacy advocates have voiced concerns on whether sharing customer data is appropriate, even in a time of crisis [23, 24]. The rapid spread of the COVID-19 at the global level highlights the need for a more harmonized, less privacy-concerning, easily accessible approach to monitoring human mobility.

The rise of social media platforms such as Twitter (twitter.com), Flickr (www.flickr.com), and Instagram (www.instagram.com) offers another possible solution to closely monitoring human mobility changes, thanks to the timely geospatial information from the enormous sensing network constituted by millions of users. The huge volume of user-generated content from

social media platforms greatly facilitates the real-time or near real-time monitoring of human mobility, providing timely data of how people respond to the COVID-19 pandemic geographically, especially within different epidemic phases. The advantages of social media with respect to the aforementioned sources of digital information are that they are extensive (covering large spatial areas), easily accessible, with less privacy concern, and at low cost [25–28]. Extracting useful information from social media is not new, as the valuable geospatial insights from social media have been explored in a wide range of fields, including hazard mitigation [29–31], evacuation monitoring [27, 32, 33], urban analytics [34–37], and public health [38, 39], to list a few. Despite the existing applications, the potential of human mobility derived from social media data has not been fully explored. Questions like whether the mobility data from social media can quantitatively reflect the collaborative effort in fighting the COVID-19 pandemic and how it corresponds to the everchanging policies in different geographical regions deserve answers.

To answer the above questions, we focus on Twitter, a popular social media platform, and analyze over 580 million tweets from all over the world to see how the worldwide collaborative efforts in reducing mobility are reflected from this user-generated information in three different scales: global scale, country scale, and Conterminous U.S. (CONUS) state scale. We propose two types of distance, respectively termed as single-day distance and cross-day distance, to quantify different aspects of public mobility observed from Twitter. We further normalize these distances by setting up their corresponding baselines. The baseline mobility values are calculated for each region separately (globe, countries, and U.S. states) using data collected before strict mobility-reducing measures are implemented. To quantify the responsiveness in certain geographic regions within different epidemic phases, we propose a mobility-based responsive index (MRI) to capture the overall degree of mobility changes in response to the COVID-19 pandemic within a specific time window. Finally, we contextualize the mobility dynamics derived from Twitter with detailed measures from local authorities to shed light on their effectiveness. The theoretical, methodological, and contextual knowledge in this study is expected to inspire future applications of these easily accessible, less privacy-concerning, highly spatiotemporal data.

2. Datasets and computing environment

We collect a total of 583,748,902 geotagged tweets from 10,324,191 unique Twitter users using the official Twitter Streaming Application Programming Interface (API), comprising a five-month period from January 1, 2020 to May 31, 2020. These tweets are stored and queried in a tweet repository managed in an in-door Hadoop cluster with 13 servers using Apache Hive and Impala. A geotagged tweet is a Twitter post with embedded geolocation in the format of exact coordinates (latitude and longitude) from the device's GPS or placenames (e.g., state, county, city). While the locational accuracy of a geotagged tweet varies, depending on the settings of the account and how a user chooses to share his/her location, we exclude the tweets that are geotagged with spatial resolution lower than the city level to increase the accuracy and credibility of the mobility pattern. Following Martin et al. [40], we filter out the non-human tweets (e.g., automated weather reports, job offers, and advertising) by checking the tweet source from which application a tweet is posted. For example, tweets automatically posted for job offers from the source TweetMyJOBS and CareerArc are removed. After the filtering, a total of 496,068,100 tweets remain from 9,502,266 unique Twitter users (details of the user count with the number of tweets posted per day can be found in the S2 Fig). The computation of travel distance requires locational information from at least two positions. Thus, only users who post tweets on two consecutive days are included in the calculation of cross-day distance,

a measure that quantifies displacement between two consecutive days (details in Section 3.1). For the single-day distance, a measure that highlights the daily travel pattern, only users who post at least twice a day are included in the calculation (details in Section 3.1). In our dataset, 53.7% of users tweet at least twice a day (for the calculation of single-day distance), while 49% of users tweet cross-day (for the calculation of cross-day distance). Note that all distances computed in this study are Great Circle distances.

3. Methods

3.1 Single-day distance and cross-day distance

To quantify daily human mobility from collected Twitter data, we propose two different types of distance, respectively referred to as single-day distance (D_{sd}) and cross-day distance (D_{cd}). The concepts of the two distances are presented in Fig 1. To reduce the computational complexity, the calculation of D_{sd} is adopted and modified from Warren and Skillman [41]. In general, D_{sd} represents the users' daily maximum travel distance of all locations relative to the initial location. Its calculation is confined within a single day so that users' daily travel patterns can be revealed. Different from D_{sd}, D_{cd} measures the mean center shift between two consecutive days.

For a selected Twitter user i, let $P_{i,j}^m = \{P_{i,j}^1, P_{i,j}^2, \ldots, P_{i,j}^n\}$ denote the collection of locations derived from his/her tweets within a certain day j. Among the total of n locations in day j, $P_{i,j}^1$ denotes the initial location and $P_{i,j}^m$ always precedes $P_{i,j}^{m+1}$ in time. To compute D_{sd}, a collection of location pairs (A) is first formed by coupling $P_{i,j}^m$ with the initial location $P_{i,j}^1$, i.e., A = $\{(P_{i,j}^1, P_{i,j}^2),(P_{i,j}^1, P_{i,j}^3),\ldots(P_{i,j}^1, P_{i,j}^n)\}$. The Great Circle Distance (GCD) is applied to compute the distance of each location pair within collection A. For a given location pair $(P_{i,j}^1, P_{i,j}^m)$, their GCD can be represented as $GCD_{i,j}^{1,m}$. D_{sd} for user i in day j, referred to as $D_{sd_{i,j}}$, is computed by selecting the maximum value of $GCD_{i,j}^{1,m}$, i.e., $D_{sd_{i,j}} = max\{GCD_{i,j}^{1,2}, GCD_{i,j}^{1,3}, \ldots, GCD_{i,j}^{1,n}\}$. To compute D_{cd}, for a collection of locations from user i in day j, i.e., $\{P_{i,j}^1, P_{i,j}^2,\ldots,P_{i,j}^n\}$, a mean center ($\bar{P}_{i,j}$) is first calculated by respectively averaging the coordinates of locations in

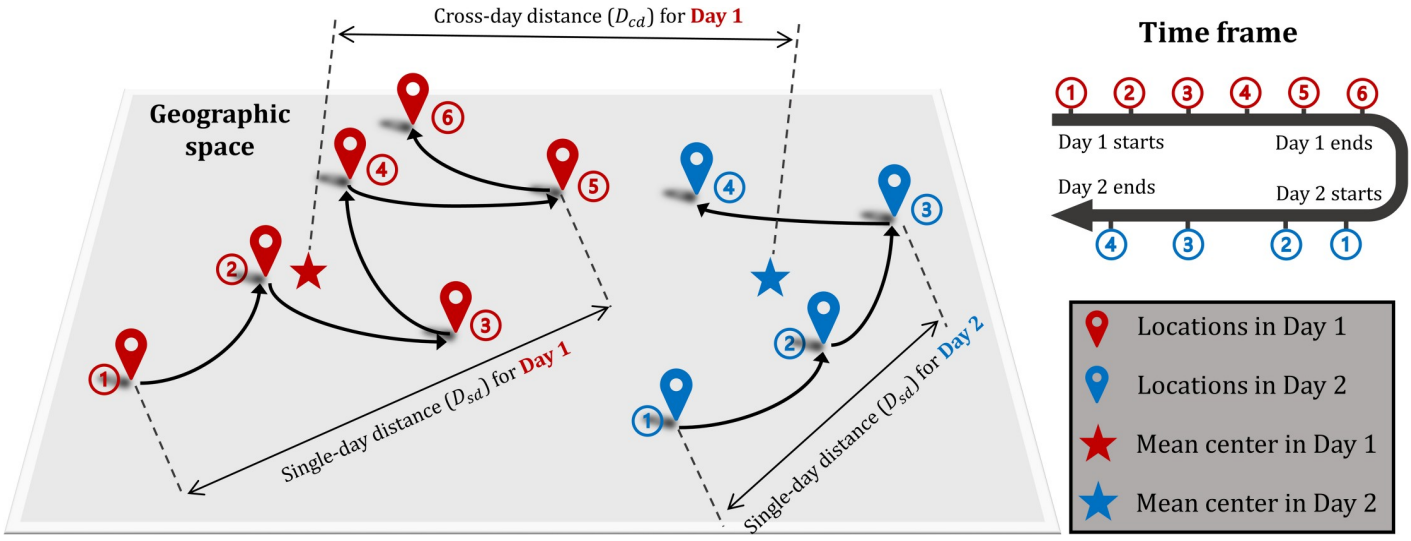

Fig 1. Conceptualization of single-day distance (D_{sd}) and cross-day distance (D_{cd}).

https://doi.org/10.1371/journal.pone.0241957.g001

$\{P^1_{i,j}, P^2_{i,j}, \ldots, P^n_{i,j}\}$:

$$\bar{P}_{i,j} = \mu\{P^1_{i,j}, P^2_{i,j}, \ldots, P^n_{i,j}\} \quad (1)$$

where $\bar{P}_{i,j}$ denotes the mean center for user i in day j and μ denotes the mean center operator. D_{cd} for user i in day j, referred to as $D_{cd_{i,j}}$, is the GCD between $\bar{P}_{i,j}$ and $P_{i,j+1}$.

Intuitively, D_{sd} and D_{cd} represent different aspects of mobility with D_{sd} measuring maximum single-day travel distance and D_{cd} measuring cross-day displacement. The dynamics of D_{sd} and D_{cd} are expected to reflect on how the COVID-19 pandemic affects people's mobility patterns geographically, presumably indicating the regional degree of responsiveness.

3.2 Normalized mobility index

Inspired by the methodological design in mobility reports from Google (www.google.com/covid19/mobility) and Apple (www.apple.com/covid19/mobility), we set up baselines for D_{sd} and D_{cd} respectively. Unlike studies that utilize a single baseline value summarized from a fixed period, our mobility baselines are set for each corresponding day of a week, as a week has been widely recognized as an independent cycle in mobility [25, 42]. That is to say, we calculate a total of fourteen baseline values, seven for D_{sd} and seven for D_{cd}, corresponding to each day of a week. For a geographical region $\mathbb{R}$ (globe, a country, or a state), let $D^{\mathbb{R}}_{sd_j}$ and $D^{\mathbb{R}}_{cd_j}$ represent the D_{sd} and D_{cd} of $\mathbb{R}$ in day j, respectively. We define that $D^{\mathbb{R}}_{sd_j}$ is the mean value of all $D^{\mathbb{R}}_{sd_{i,j}}$ in day j, i.e., $D^{\mathbb{R}}_{sd_j} = \frac{\sum_i D^{\mathbb{R}}_{sd_{i,j}}}{N}$, where N denotes the total number of selected users in day j within $\mathbb{R}$ and $P^1_{i,j} \epsilon \mathbb{R}$. Similarly, $D^{\mathbb{R}}_{cd_j}$ is the mean value of all $D^{\mathbb{R}}_{cd_{i,j}}$ in day j, i.e., $D^{\mathbb{R}}_{cd_{i,j}} = \frac{\sum_i D^{\mathbb{R}}_{cd_{i,j}}}{N}$, where $\bar{P}_{i,j} \epsilon \mathbb{R}$. Consequently, the normalized mobility index of region $\mathbb{R}$ in day j for single-day distance ($NMI^{\mathbb{R}}_{sd_j}$) and cross-day distance ($NMI^{\mathbb{R}}_{cd_j}$) are respectively defined as the ratios of $D^{\mathbb{R}}_{sd_j}$ and $D^{\mathbb{R}}_{cd_{i,j}}$ to their baseline values of a corresponding day in a week. Given their calculations, $NMI^{\mathbb{R}}_{sd_j}$ and $NMI^{\mathbb{R}}_{cd_j}$ both have a range of $[0,+\infty)$, with 1 being the critical value. When the $NMI^{\mathbb{R}}_{sd_j}$ (or $NMI^{\mathbb{R}}_{cd_j}$) is less than 1, it suggests that within region $\mathbb{R}$ in day j, reduced mobility is observed compared with the baseline mobility when measuring single-day distance (or cross-day distance).

3.3 Mobility-based responsive index

After the normalization in the previous section, a baseline of NMI (i.e., $NMI = 1$) that separates patterns of increased mobility and reduced mobility is formed. Intuitively, for a time series of NMI values, the size of the area under the NMI baseline (S_{AUB}) represents the degree of positive responses (i.e., reduce in mobility) for a given period, while the size of the area above the NMI baseline (S_{AAB}) indicates otherwise (Fig 2). Hypothetically, the area in perfect condition (S_{APC}) represents a perfect scenario where mobility instantly reduced to 0 from the beginning and remains 0 until the time series ends. Apparently, such a scenario is purely theoretical and certainly does not exist in the real world. However, it provides a baseline where other scenarios are compared against, facilitating the quantification of how close other scenarios are compared to the perfect scenario. Conceptually, the mobility-based responsive index we propose is the ratio between the net positive response to the perfect scenario, i.e., $\frac{\sum S_{AUB} - \sum S_{AAB}}{S_{APC}}$, where ΣS_{AUB} and ΣS_{AAB} respectively denote the summation of areas under the curve and the summation of areas above the curve, given a specific period.

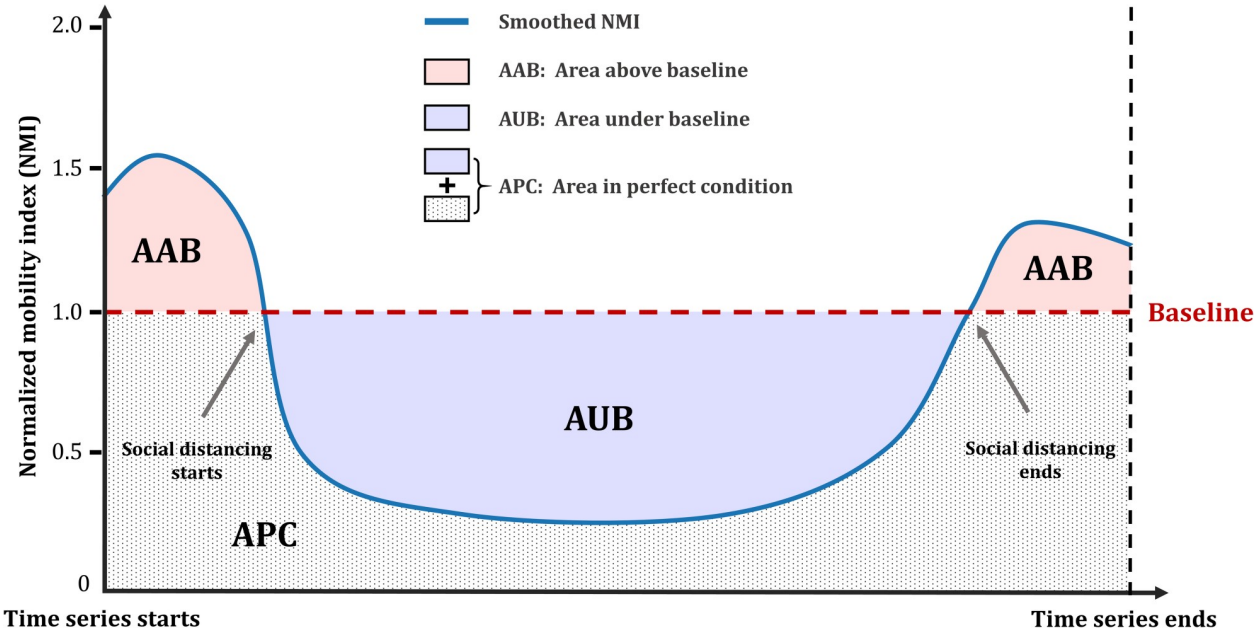

Fig 2. Mobility-based responsive index.

https://doi.org/10.1371/journal.pone.0241957.g002

To remove noises and reveal the general trend, we smooth the time series using a one-dimensional Gaussian filter ($\sigma = 2$), one of the most popular filters widely applied in many temporal smoothing tasks [43, 44]. Further calculations regarding the size of the areas are all based on the smoothed time series. Given the different nature of the two proposed distances, we calculate their *MRI* separately:

$$MRI_{sd} = \frac{\sum S_{AUB_{sd}} - \sum S_{AAB_{sd}}}{S_{APC}} \tag{2}$$

$$MRI_{cd} = \frac{\sum S_{AUB_{cd}} - \sum S_{AAB_{cd}}}{S_{APC}} \tag{3}$$

where MRI_{sd} and MRI_{cd} denote the *MRI* with D_{sd} and D_{cd} being measured, respectively. We further compute an integrated *MRI* by weighting MRI_{sd} and MRI_{cd} using their total sample sizes:

$$MRI = \frac{MRI_{sd} \times u_{sd} + MRI_{cd} \times u_{cd}}{u_{sd} + u_{cd}} \tag{4}$$

where u_{sd} and u_{cd} denote the total sample sizes used to calculate MRI_{sd} and MRI_{cd}, respectively. Intuitively, MRI_{sd} captures the mobility responsiveness confined in a single day, revealing the dynamics of daily travel patterns while MRI_{cd} captures the mobility responsiveness between two consecutive days, revealing the dynamics of cross-day travel patterns. The rationale of deriving an integrated *MRI* by fusing MRI_{sd} and MRI_{cd} is that, despite their different calculations, they reflect human mobility from diverse perspectives, and therefore their integration serves as an overall index that better summarizes the general degree of mobility-based responsiveness geographically. The derived *MRI* has a range of $(-\infty,1]$. In general, the higher the value, the better responsiveness a region has, with $MRI = 1$ suggesting hypothetically perfect

responsiveness. A positive *MRI* (*MRI*>0) suggests positive responsiveness (reduce in mobility) for a region, while a negative one suggests otherwise.

4. Results

4.1 Global scale

As most countries in the world started to aggressively respond to the COVID-19 pandemic after March, 2020, we set our baselines in a temporal period from January 13, 2020 (to exclude abnormal mobility patterns due to the New Year holiday season) to February 29, 2020. Since the outbreak in China and the dramatic increase in cases in Europe, many countries have imposed and continue to impose travel bans and lockdowns [45]. As a result, both D_{sd} and D_{cd} have greatly deviated from their corresponding baselines, especially after March 11, 2020, when WHO declared COVID-19 as a pandemic (Fig 3). Because both our baselines are set for the individual day in a week, their projections exhibit a clear weekly pattern. In comparison, the time series of D_{sd} and D_{cd}, especially after the declaration of COVID-19 as a pandemic, show considerably less periodicity (Fig 3), suggesting that the protection measures (e.g., travel restrictions, social distancing policies, stay-at-home orders) have obviously affected people's weekly routines. The gap between baselines proves the different nature of D_{sd} and D_{cd}, well explaining our rationale of normalizing D_{sd} and D_{cd} separately. We further observe that, throughout the entire time series, the daily value of D_{cd} is considerably lower than the daily value of D_{sd}. This phenomenon can be explained by the existence of a large amount of Twitter users who, despite their large single-day travel distance (high D_{sd} value), keep a similar daily posting routine, which leads to no significant shift of mean centers between two consecutive days (low D_{cd} value).

We observe similar mobility dynamics when D_{sd} and D_{cd} are respectively normalized to NMI_{sd} and NMI_{sd} according to their baselines (Fig 4). Both NMI_{sd} and NMI_{sd} started to deviate from the baseline (NMI = 1) around ten days before the pandemic declaration from the WHO, suggesting that strong mobility-reducing measures had been taken before the declaration on March 11, 2020. This mobility pattern coincides with strong early travel restrictions implemented in Europe and Asia at the beginning of March [6, 46]. At the end of March, both NMI_{sd} and NMI_{cd} reached the bottom with the lowest NMI_{sd} = 0.70 and the lowest NMI_{cd} = 0.45, indicating that single-day distance and cross-day distance respectively reduced to 70% and 45% of the ones in the normal situation. Starting from the end of April, however, both

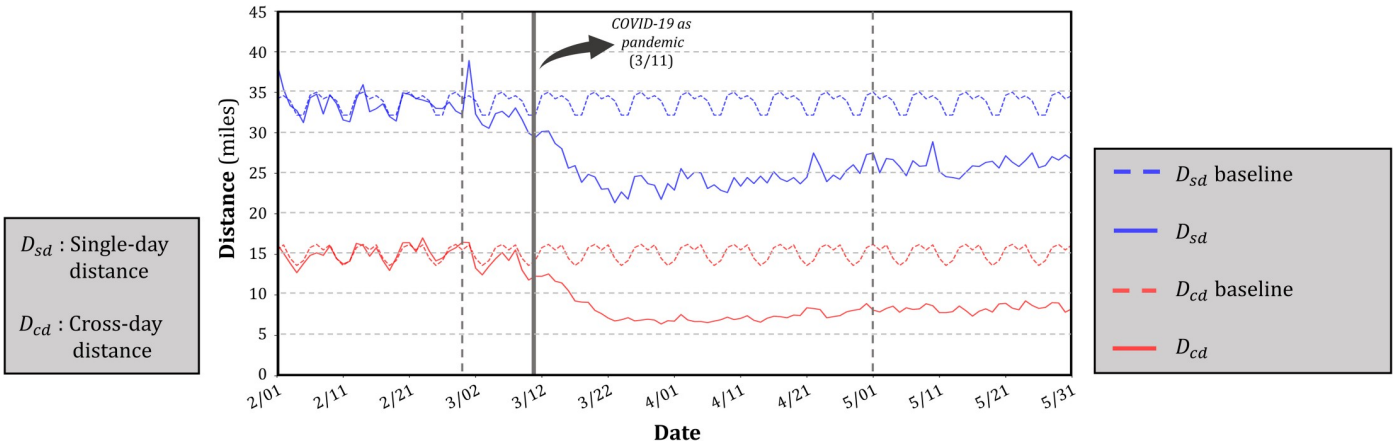

Fig 3. Temporal distribution of global D_{sd} and D_{cd} in the four-month period (February, March, April, and May).

https://doi.org/10.1371/journal.pone.0241957.g003

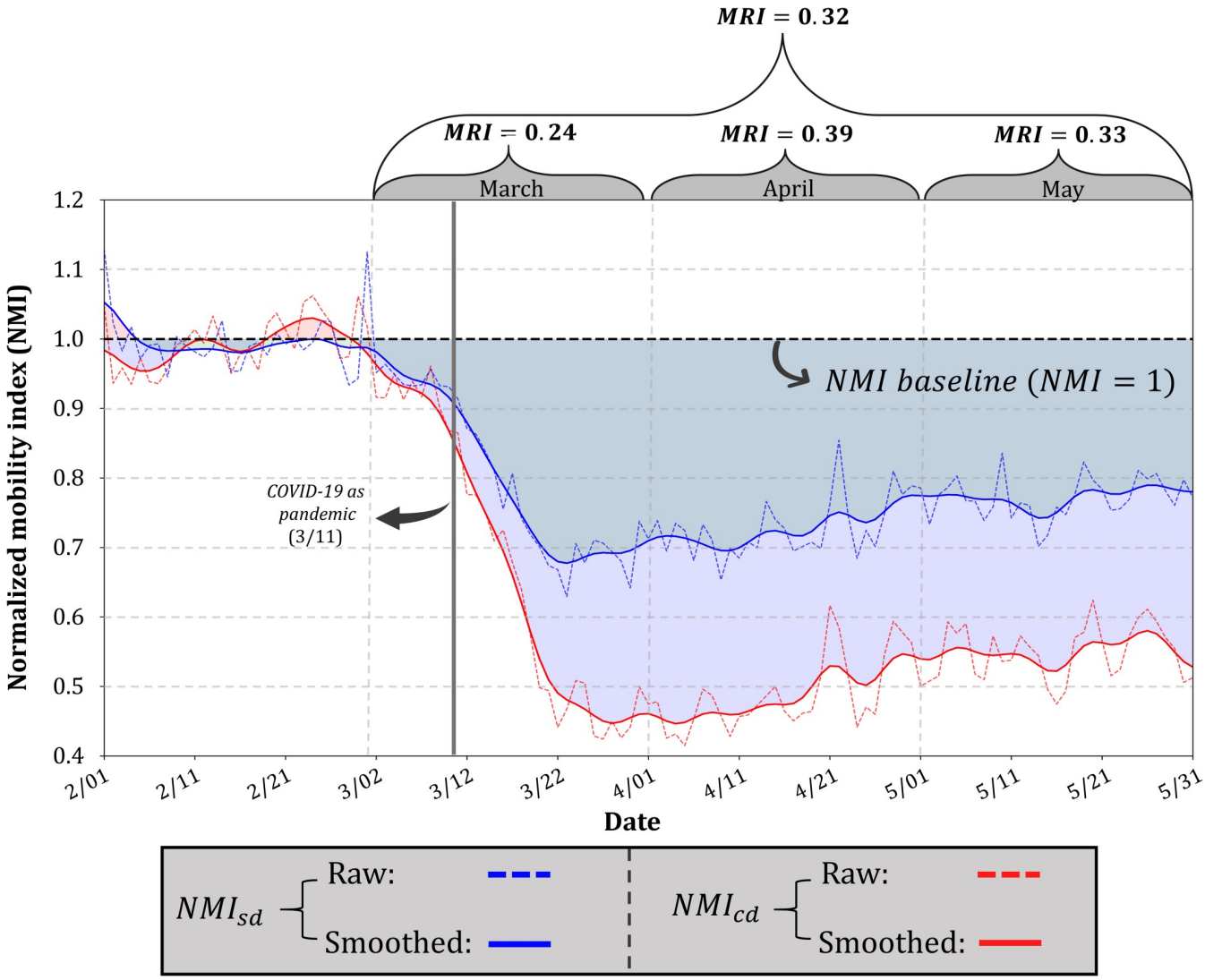

Fig 4. Global NMI_{sd} (normalized D_{sd}) and NMI_{cd} (normalized D_{cd}) in the four-month period, and the monthly MRI for March, April, and May.

https://doi.org/10.1371/journal.pone.0241957.g004

NMI_{sd} and NMI_{cd} started to bounce back, and the increasing trend continued to the end of May, presumably resulting from the gradually lifted quarantine measures [47]. Compared with the hypothetically perfect scenario ($MRI = 1$) where mobility instantly halts and remains 0 throughout the time series, the overall *MRI* for the three-month combined is 0.32, and the *MRIs* for the March, April, and May, respectively are 0.24, 0.39, and 0.33, revealing the less responsiveness in May compared with April.

4.2 Country scale

For country scale study, we set the mobility baseline in a period from January 13, 2020 to February 15, 2020, as some countries (e.g., Italy and South Korea) already imposed strict or voluntary mobility-reducing policies as early as in late-February. To ensure that Twitter records are sufficient enough to generate a reasonable and stable time series, we mainly target the top 20 countries with most Twitter users, according to the Digital 2020 April Global Statshot Report [48]. The selection of those countries mostly agrees with the Twitter data we collected.

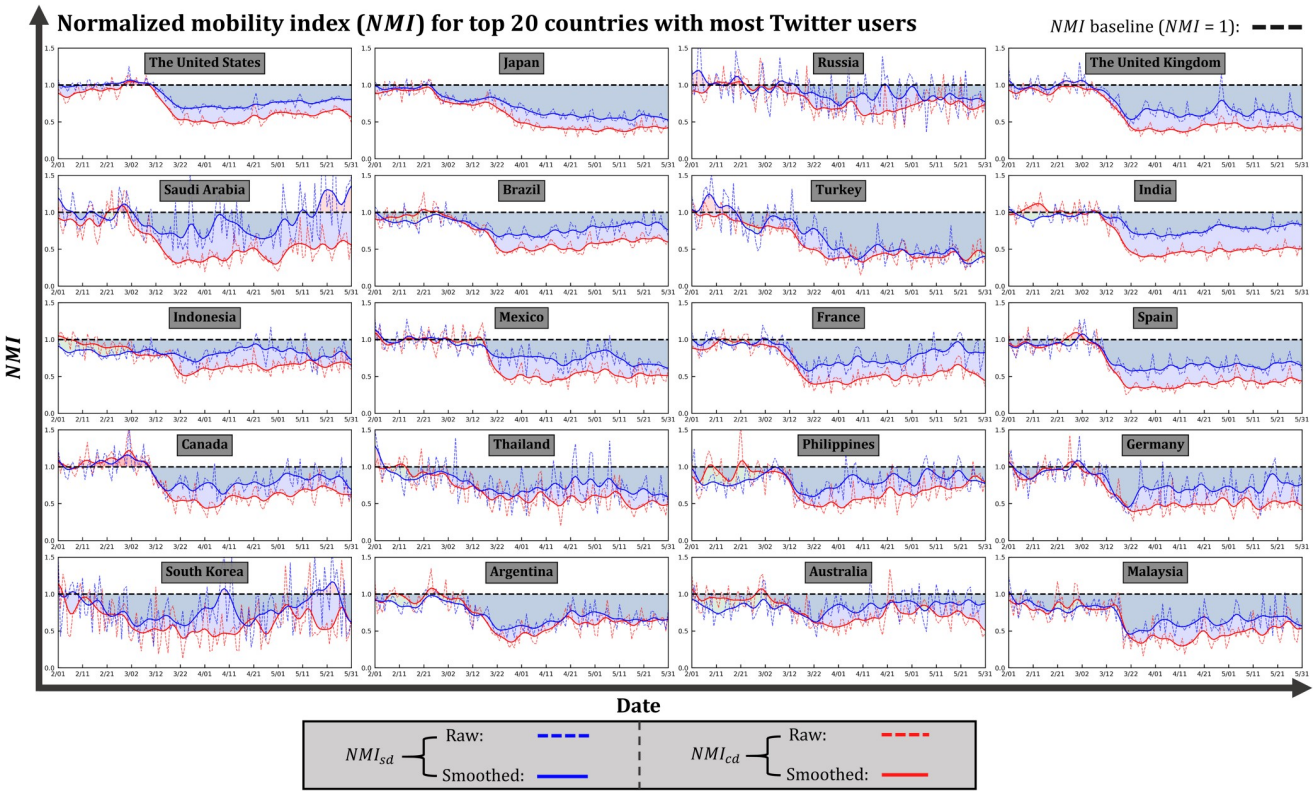

Fig 5. Temporal distribution of NMI_{sd} and NMI_{cd} for the top 20 countries with most Twitter users in February, March, April, and May.

https://doi.org/10.1371/journal.pone.0241957.g005

In general, the impact of the COVID-19 pandemic on mobility derived from Twitter is obvious, as the mobility of the selected 20 countries, measured by single-day distance and cross-day distance, is mostly below the mobility baseline in March, April, and May (Fig 5), suggesting that mobility-reducing measures have been suggested and adopted in those countries. However, the country-level discrepancies in the time series of NMI_{sd} and NMI_{cd} can be clearly observed. The mobility in Japan started to drop in late-February (Fig 5), presumably in response to the announcement by Prime Minister Shinzo Abe on February 27, 2020 to close all Japanese elementary, junior high, and high school [49]. The further decline of mobility from early-April to late-April can be explained by the proclamation of the State of Emergency for Tokyo (April 7) and for the rest of the country (April 16) [50]. The mobility of Japan is expected to bounce back, as Japan ended the state of emergency in all of Japan On May 25, 2020 [51]. Given the limited temporal coverage of our data, however, its impact on mobility remains unknown. The mobility of the United States started to drop in mid-March when a series of statements were announced, including the declaration of COVID-19 as a pandemic by the WHO (March 11) and the declaration of National Emergency by the White House (March 13, 2020). The mobility remained consistently low in April, then gained an upward momentum in May, largely due to the gradually loosened measures [52]. A similar mobility pattern can also be observed in India, where mobility reduced following the WHO's declaration in mid-March and gradually rose in May. Mobility in Malaysia was slightly below the baseline in late-February and early-March. The sudden mobility drop appeared on March 18, which coincides with the date when the Movement Control Order (MCO) from the federal government took effect [53]. The rapid mobility reduction in Malaysia demonstrates that the

Table 1. Mobility-based responsive index (*MRI*) for the top 20 countries with most Twitter users.

Country names	*MRI*					
	Mar	Apr	May	Three-month average	∇(Apr-Mar)	∇(May-Apr)
Argentina	0.32	0.39	0.35	0.35	0.07	-0.04
Australia	0.23	0.22	0.20	0.22	-0.01	-0.02
Brazil	0.25	0.38	0.27	0.30	0.13	-0.11
Canada	0.21	0.35	0.23	0.26	0.14	-0.12
Germany	0.32	0.39	0.37	0.36	0.07	-0.02
Spain	0.32	0.49	0.45	0.42	0.17	-0.04
France	0.31	0.41	0.29	0.34	0.1	-0.12
The United Kingdom	0.27	0.48	0.47	0.41	0.21	-0.01
Indonesia	0.24	0.25	0.26	0.25	0.01	0.01
India	0.21	0.40	0.35	0.32	0.19	-0.05
Japan	0.25	0.49	0.53	0.42	0.24	0.04
South Korea	0.44	0.35	0.20	0.33	-0.09	-0.15
Mexico	0.16	0.38	0.38	0.31	0.22	0.00
Malaysia	0.34	0.50	0.40	0.41	0.16	-0.1
Philippines	0.28	0.28	0.20	0.25	0.00	-0.08
Russia	0.12	0.23	0.20	0.18	0.11	-0.03
Saudi Arabia	0.36	0.41	0.23	0.33	0.05	-0.18
Thailand	0.30	0.34	0.39	0.34	0.04	0.05
Turkey	0.29	0.57	0.60	0.49	0.28	0.03
The United States	0.20	0.38	0.29	0.29	0.18	-0.09

https://doi.org/10.1371/journal.pone.0241957.t001

MCO was effectively and efficiently executed. In Saudi Arabia, mobility started to reduce as early as March 2, when the first case was confirmed [54]. However, NMI_{sd} and NMI_{cd} gradually diverged as NMI_{cd} remained stably low in April and May, while NMI_{sd} became unstable and eventually recovered and even surpassed baseline mobility in mid-May. The divergence in trends of the two types of distances can be partially explained by the suspension of flights and mass land transport (trains, buses, and taxis) that took effect on March 21 [55]. The lack of public transit is responsible for the consistently low cross-day distance.

Compared with the hypothetically perfect scenario, i.e., *MRI* = 1, Turkey has the highest three-month *MRI* (0.49), followed by Spain (0.43), Japan (0.42), Malaysia (0.41), and the U.K. (0.41) (Table 1). Russia has the lowest three-month *MRI* (0.18), followed by Australia (0.22), Indonesia (0.25), Philippines (0.25), Canada (0.26), and the U.S. (0.29) (Table 1). The high *MRI* (0.44) of March in South Korea, a country that suffered from the initial spread of the epidemic in its early stage besides China, indicates that the early and strong mitigation measures were announced and implemented effectively. In light of the gradually easing situation [56], the social distancing measures in South Korea started to be lifted, evidenced by the fact that its *MRI* decreased respectively by 0.09 and 0.15 in April and May. In the U.S., the mobility-based responsiveness in March (0.20) is among the weakest in the 20 selected countries (Table 1). In April, the *MRI* of the U.S. reached 0.38, a net gain of 0.18 compared to the *MRI* in March. The strong responsiveness of mobility in April is largely due to the gradually issued statewide stay-at-home orders since late-March that eventually affected at least 316 million people in at least 42 states [57]. With the lifting of orders in late-April and May, however, the U.S. showed reduced responsiveness, evidenced by its 0.09 loss in *MRI* of May compared to April. As the U.S. has become the new COVID-19 epicenter, the reduced mobility responsiveness, along with the rocketing number of confirmed cases, deserves more attention.

Besides the countries presented in Fig 5, the temporal distribution of NMI_{sd} and NMI_{cd} for the other 16 countries with relatively fewer Twitter samples can be found in the S1 Fig. Information regarding the accumulated user count for distance calculation (both D_{sd} and D_{cd}) in selected countries is presented in the S1 Table.

4.2 States in the CONUS

Given that the first State of Emergency related to COVID-19 in the U.S. was declared by Washington State (WA) on February 29, 2020, while the majority of the states started to react aggressively after mid-March, we set the U.S. mobility baseline in a period from January 13 to February 29, 2020. In general, the influence of the COVID-19 pandemic on mobility is distinct, as the drop of mobility in most of the states happened in mid-March (Fig 6), potentially triggered by the events that include the pandemic declaration (March 11) and the National Emergency declaration (March 13). Although social distancing guidelines that aim to curb the spread have been suggested in the entire nation, the impacts varied substantially among states (Fig 6). Heavily hit states, e.g., NY, NJ, IL, CA, MA, and PA, generally experienced sharp mobility reduction, and their mobility remained stably low since mid-March. States with low numbers of cases, e.g., DE, MT, ME, WV, SD, and WY, despite the fluctuations in their time series, exhibited relatively marginal mobility reduction compared with heavily hit states. As the first state to announce the State of Emergency at the end of February, the mobility in WA remained close to the baseline in early March. It was not until mid-March that the mobility of WA started to noticeably decrease, which potentially indicates that the early mitigation policies

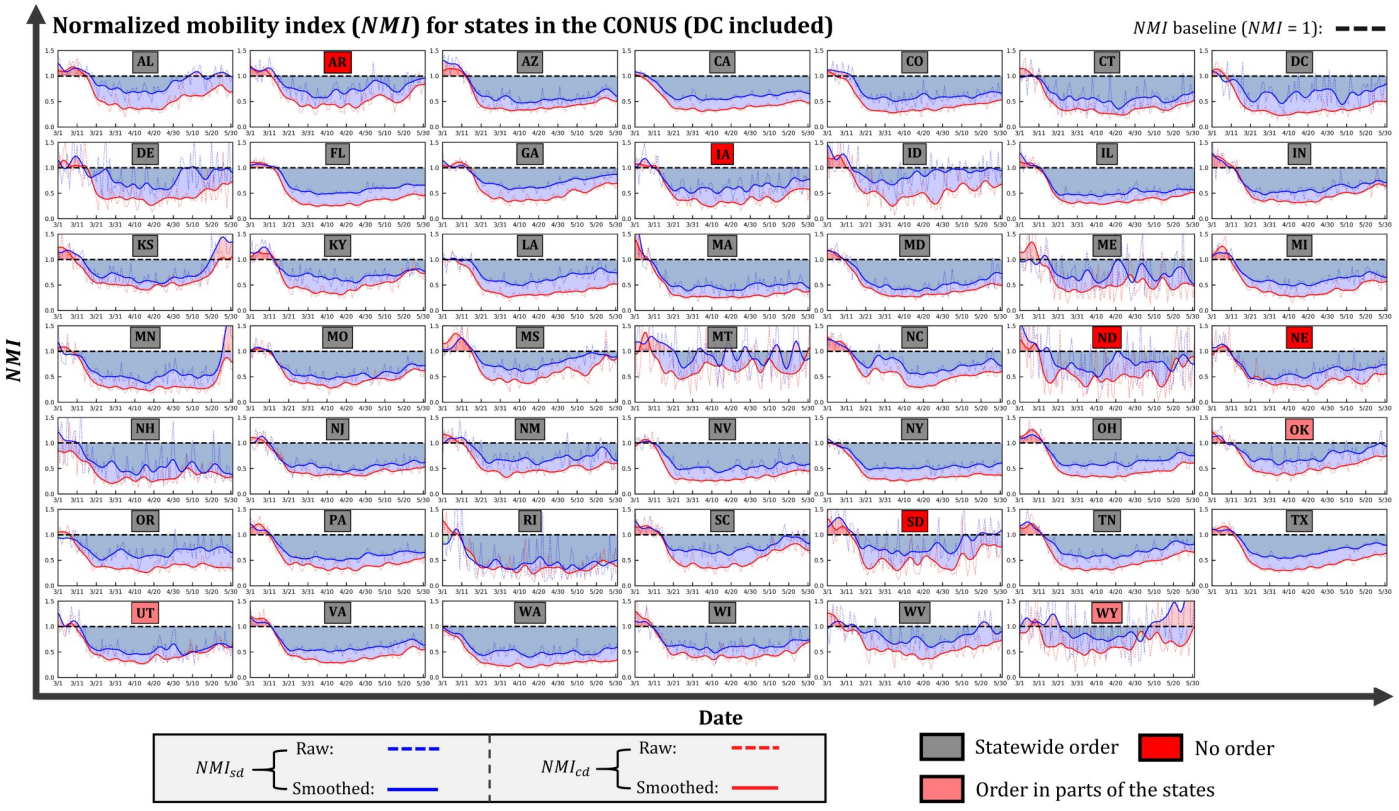

Fig 6. Temporal distribution of NMI_{sd} and NMI_{cd} for states in CONUS (DC included; VT not included) in March, April, and May.

https://doi.org/10.1371/journal.pone.0241957.g006

in WA were not implemented effectively. The time series of mobility in states that include KS, MN, MS, AL, WV, SC, and WY, presents a bowl-shaped pattern, suggesting the strong recovery of mobility with some even bouncing beyond the baseline due to the gradually loosened measures. In response to the COVID-19 pandemic, eight states, including AR, IA, ND, NE, SD, UT, OK, and WY, decline to impose statewide stay-at-home orders by favoring other restrictions [57]. Without the orders, however, the aforementioned states still present considerable mobility reduction amid the pandemic, indicating the effectiveness of the federal guidelines and other mitigation approaches from the local government. Given the insufficient samples in the calculation of the baseline mobility, the mobility pattern in VT is not presented in Fig 6. The state names associated with their abbreviations and the accumulated user count for distance calculation in each state are presented in the S2 Table.

In late-May, the risk of transmission in the U.S. was further complicated by the protests demanding justice after Mr. George Floyd died following an altercation with police. A noticeable mobility increase following the incident can be found in MN, where the incident happened (Fig 7). Carried by the existed mobility recovering momentum in mid-May, MN saw a significant increasing trend in both NMI_{sd} and NMI_{cd} at the end of the time series. A distinct spike can be found on May 29, 2020, when the raw NMI_{sd} and raw NMI_{sd} all went beyond the baseline, with the NMI_{sd} (representing single-day maximum travel distance) reaching about 2.5 times than usual as a consequence of the increased activity during the protests. The divergent functionality of the smoothed *NMI* and the raw *NMI* is well illustrated, as the former highlights the general trend while the latter is able to capture the spikes caused by disruptive events. At the time of writing, the protests have gradually spread across the U.S. and even overseas. The increase in mobility resulting from the protests deserves close monitoring, as standing in a crowd for long periods undoubtedly raises the risk of increased transmission and further worsens the situation.

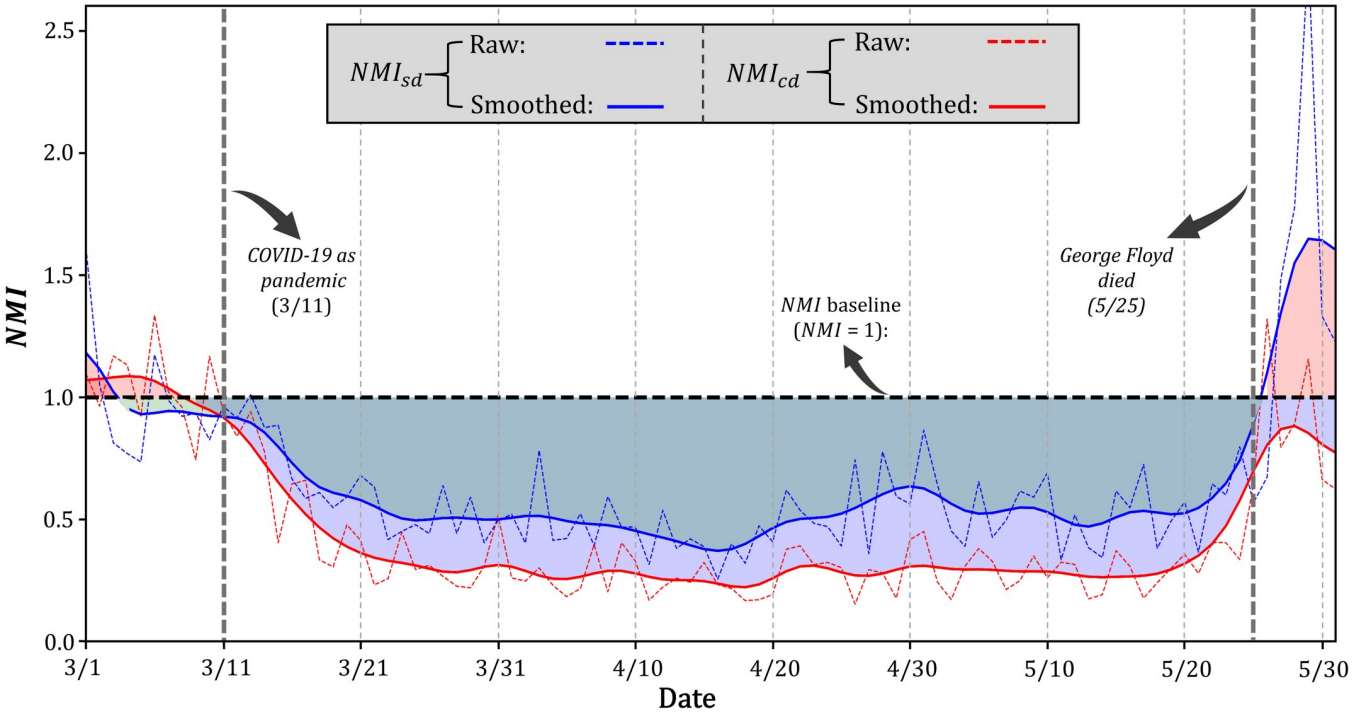

Fig 7. Temporal distribution of NMI_{sd} and NMI_{cd} for Minnesota.

https://doi.org/10.1371/journal.pone.0241957.g007

The monthly *MRI* at the state level further highlights the responsiveness of each state in the three-month period. As expected, states with early spikes of cases and early strong mitigation policies tend to have a higher *MRI* in March (Fig 8). WA (0.41) leads the *MRI* in March, followed by NY (0.33), NH (0.32), and MA (0.32) (Table 2). The high responsiveness at the early stage suggests that the mobility-reducing guidelines were implemented timely and efficiently in those states. In April, the responsiveness in all the states continued to strengthen (Fig 8), given the rising of cases and gradually tightened measures (Table 2). From March to April, MD, FL, and MI are the top three states with the most increase of *MRI*, respectively by 0.42, 0.41, and 0.39 (Table 2). The significant boost of mobility-based responsiveness reflects not only the severity of the situation but also the strong implementation of the mitigation measures. However, with the lifting of orders, 47 states (except MT) have shown reduced responsiveness in May compared to April (Fig 8). In light of the increasing number of cases in the U. S. with no sign of slowing down (at the time of writing), the reduced mobility responsiveness can potentially foster a second wave of infections. Because of the insufficient samples in the baseline calculation, the *MRI* for VT is not presented in Fig 8 and Table 2.

5. Discussion

5.1 Merits of social media data in gauging human mobility dynamics

The rise of social media platforms in recent years offers a potential solution to closely monitoring human mobility dynamics, given their real-time high-volume user-generated content. Public health crises like the COVID-19 pandemic uniquely highlight several merits of social media data. First, social media data are a more harmonized source compared to cellphone records from certain providers that differ geographically. Twitter, for example, has 330 million

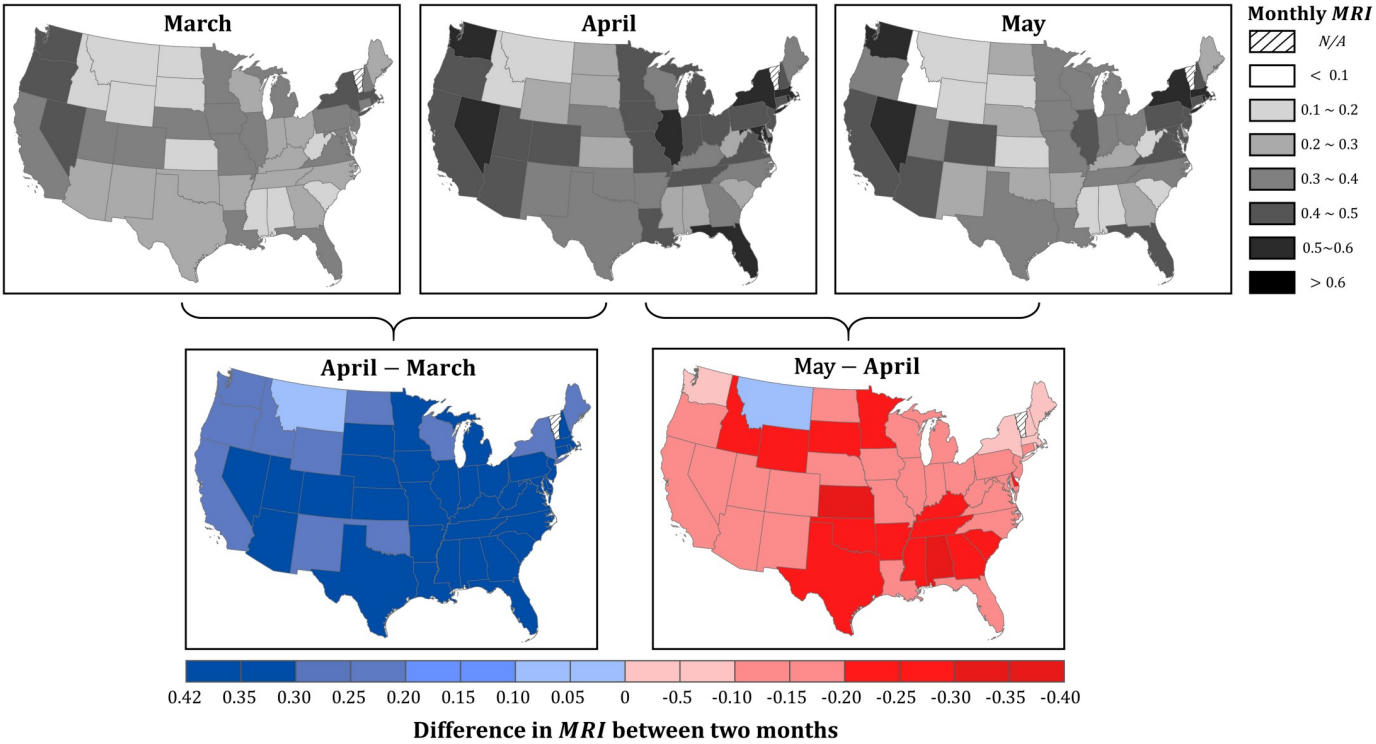

Fig 8. Mobility-based responsive index (*MRI*) for CONUS states in March, April, May, and the difference between two consecutive months. State boundaries are retrieved from the U.S. Census Bureau (https://www.census.gov/geographies/mapping-files/time-series/geo/carto-boundary-file.html).

https://doi.org/10.1371/journal.pone.0241957.g008

Table 2. Mobility-based responsive index (*MRI*) for states in the CONUS.

State abbreviations	*MRI*					
	Mar	Apr	May	Three-month average	∇(Apr-Mar)	∇(May-Apr)
AL	0.09	0.45	0.15	0.23	0.37	-0.30
AR	0.13	0.44	0.23	0.27	0.32	-0.21
AZ	0.19	0.57	0.46	0.40	0.38	-0.11
CA	0.30	0.55	0.45	0.43	0.25	-0.10
CO	0.25	0.57	0.46	0.42	0.32	-0.11
CT	0.27	0.60	0.50	0.46	0.34	-0.10
DC	0.30	0.56	0.47	0.44	0.26	-0.09
DE	0.10	0.48	0.25	0.28	0.38	-0.23
FL	0.22	0.63	0.48	0.44	0.41	-0.14
GA	0.15	0.51	0.29	0.31	0.36	-0.22
IA	0.26	0.58	0.44	0.43	0.32	-0.14
ID	0.07	0.36	0.15	0.19	0.29	-0.21
IL	0.24	0.60	0.50	0.45	0.35	-0.10
IN	0.19	0.55	0.36	0.37	0.36	-0.19
KS	0.14	0.45	0.15	0.25	0.32	-0.30
KY	0.16	0.51	0.30	0.32	0.35	-0.20
LA	0.18	0.55	0.37	0.37	0.37	-0.18
MA	0.32	0.65	0.57	0.51	0.34	-0.08
MD	0.23	0.65	0.49	0.46	0.42	-0.17
ME	0.19	0.42	0.39	0.33	0.23	-0.03
MI	0.20	0.60	0.40	0.40	0.39	-0.19
MN	0.30	0.64	0.44	0.46	0.35	-0.20
MO	0.26	0.60	0.44	0.43	0.33	-0.15
MS	0.07	0.42	0.16	0.22	0.35	-0.26
MT	0.11	0.16	0.19	0.15	0.06	0.03
NC	0.11	0.47	0.36	0.31	0.36	-0.12
ND	0.10	0.36	0.25	0.24	0.26	-0.11
NE	0.23	0.56	0.40	0.40	0.34	-0.16
NH	0.32	0.64	0.57	0.51	0.31	-0.07
NJ	0.23	0.57	0.46	0.42	0.33	-0.11
NM	0.15	0.45	0.32	0.31	0.30	-0.13
NV	0.30	0.63	0.53	0.48	0.33	-0.10
NY	0.33	0.62	0.55	0.50	0.29	-0.07
OH	0.16	0.53	0.38	0.36	0.37	-0.16
OK	0.18	0.45	0.23	0.29	0.27	-0.22
OR	0.30	0.54	0.43	0.42	0.24	-0.10
PA	0.22	0.57	0.46	0.42	0.35	-0.12
RI	0.30	0.63	0.62	0.52	0.33	-0.01
SC	0.11	0.45	0.18	0.25	0.34	-0.27
SD	0.11	0.42	0.21	0.24	0.31	-0.20
TN	0.16	0.54	0.31	0.34	0.37	-0.22
TX	0.20	0.55	0.34	0.36	0.35	-0.20
UT	0.27	0.59	0.47	0.44	0.32	-0.12
VA	0.22	0.58	0.43	0.41	0.35	-0.14
WA	0.41	0.66	0.61	0.56	0.25	-0.05
WI	0.22	0.51	0.42	0.38	0.30	-0.10

(*Continued*)

Table 2. (Continued)

State abbreviations	*MRI*					
	Mar	Apr	May	Three-month average	∇(Apr-Mar)	∇(May-Apr)
WV	0.07	0.41	0.23	0.24	0.34	-0.18
WY	0.13	0.34	0.05	0.18	0.22	-0.29

Note. VT (Vermont) is not included due to the insufficient samples in baseline calculation.

https://doi.org/10.1371/journal.pone.0241957.t002

monthly active users and 500 million daily posts worldwide [58]. Its popularity allows it to serve as a valuable venue where derived mobility dynamics can be cross-compared in different regions, especially for a global epidemic event like the COVID-19. Second, social media data offer both immediacy and spatially explicit geo-information that traditional approaches like surveys and censuses are often not capable of. The rapid spread of the SARS-CoV-2 virus and the everchanging mitigation policies greatly magnify the merit of timeliness in real-time crowdsourcing platforms, including social media. Third, social media data are relatively less privacy-concerning compared to passive data-collecting approaches that include phone calls, cellular records, and smart cards. The privacy issues in the above passive methods preclude the analysis in a more spatial explicit manner, as data collected via those methods are usually de-identified and aggregated before application. Finally, despite the required computational resources and storage that are essential to handle the large volume and velocity of Twitter data, such data are easily accessible and cost-efficient. In these respects, geotagged tweets can and should be considered as a valuable proxy for human mobility, especially during times of crisis (like the COVID-19 pandemic we are facing) that usually cause dramatic mobility changes.

5.2 Limitations

The results of this study should be interpreted in light of several important limitations. First, the representativeness of Twitter data may not reflect the characteristics of the population as a whole in terms of socioeconomic status, age, gender, or race. Furthermore, the representativeness may vary geographically. Despite the attempts to improve the understanding of the demographics of Twitter users via profile scrutiny and tweets mining [27, 59], the intrinsic biases in Twitter samples should be considered when the results of this study are interpreted. The problem of representativeness, however, exists in all digital services. Mobility patterns derived from phone calls and cell phone applications (e.g., Google Maps and Apple Maps) also have to face the criticisms that people left behind by the "Digital Divide" [60] are underrepresented.

Second, the Twitter API allows unrestricted access to only about 1% of the total records [61]. From the tweets that streamed down via the Twitter API, we only use tweets that are geotagged with spatial resolution lower than the city level. Despite the "Big Data" nature of Twitter as a data source, the available records that can be used to derive human mobility patterns are still insufficient in some regions at a temporal resolution of daily. Mobility time series computed from insufficient samples tend to have more fluctuations, making the general pattern less recognizable and less reliable. In this respect, the mobility dynamics identified in the study only account for the reaction of Twitter in response to the COVID-19 pandemic and should not be generalized to infer the mobility of the total population without caution.

Third, the less privacy-concerning nature of social media data also creates many challenges. Unlikely the passively collected data from mobile telephone records, smart cards, and wireless networks, social media data own intrinsic active nature, as users must grant permission to share their data and determine the locational accuracy of their posts, all depending on their

personal settings. Thus, the two types of distances proposed in this study, single-day distance and cross-day distance, only reflect the travel behaviors that users are willing to share. This active nature protects privacy to some degree. At the same time, however, it dilutes the total amount of available trajectory data both spatially and temporally, potentially causing skewness in the extracted origin-destination information.

Finally, our mobility baseline, where mobility patterns from other periods are compared against, is derived from a one-month period that starts from mid-January. We further compute baselines for each corresponding day of a week by recognizing a week as an independent mobility cycle, without considering the monthly discrepancies that mobility patterns may present. Studies have shown that mobility may vary regularly on a monthly basis [62, 63], and the variations differ geographically due to the different cultural and societal settings. The uncertainty resulting from the short baseline period that specifically covers late-January and February needs to be acknowledged.

5.3 Future directions

Despite these limitations, we believe the strengths and valuable findings in this study outweigh the shortcomings. However, several lines of future studies are still in need. First, future work should investigate the representativeness of Twitter data by delving into the demographics of Twitter users. The mobility patterns documented in this study only reflect Twitter users' collective activities responding to the COVID-19 pandemic. Thus, the representativeness of the findings largely depends on the demographics of the local users in relation to the demographics of the local population. Another research direction is to examine the similarity and dissimilarity in mobility patterns derived from various sources (social media, phone calls, cellular records, smart cards, etc.), as they reflect human mobility from different yet valuable perspectives. Following the mathematical design in this study, we compared Twitter mobility with the Apple mobility report, the Google mobility report, and mobility data from Descartes Labs [64]. Future studies are needed to investigate the characteristics of other heterogeneous mobility sources to understand the strengths and pitfalls of each source. The third line of research is to explore the potential in the integration of mobility indices from heterogeneous data sources. An integrated mobility index from multiple sources is expected to better reflect the multifaceted nature of human mobility, thus greatly facilitating comprehensive mobility monitoring. Fourth, research on more extensive Twitter datasets is needed to investigate the possible improvement in mobility that can be captured. Although millions of spatially explicit Twitter posts collected in this study are sufficient to quantitatively reflect the human mobility dynamics during the pandemic, an increasing amount of tweets are expected to generate more stable and reliable trends with fewer random fluctuations. Despite the fact that the licenses for other sample sizes, such as Gecahose (returning 10% of the public data) and Firehose (returning 100% of the public data), are costly, difficult to obtain, and requiring a demanding computational environment [65], their potential in obtaining reliable mobility dynamics at much finer spatiotemporal resolutions deserves attention. Finally, as human population movement is among the critical dimension that drives the spatial spread of COVID-19, how to leverage such Twitter derived mobility information for better predicting the future infectious risk of a state, county, or community warrants investigation.

6. Conclusion

As the whole world is now fighting the COVID-19 pandemic, the effectiveness of mobility-reducing measures (e.g., social/physical distancing) at varying scales needs rapid investigation. This article examines the reaction in social media, specifically Twitter, spatially and temporally

in response to the COVID-19 pandemic as a more harmonized, less privacy-concerning, and cost-efficient approach to assessing human mobility dynamics promptly. Through analyzing more than 580 million tweets worldwide, we present how our collaborative efforts in mobility reduction are reflected from this user-generated information in three different geographic scales: global scale, country scale, and U.S. state scale. To quantify various aspects of mobility from Twitter, we propose two types of distance, i.e., the single-day distance that highlights daily travel behavior and the cross-day distance that highlights the displacement between two consecutive days. To facilitate the comparison with normal situations, we further normalize these distances by separately setting up their baselines for each corresponding day of a week. We also propose a mobility-based responsive index (*MRI*) to capture the overall degree of mobility-related responsiveness of particular geographic regions in response to the COVID-19 pandemic.

The results suggest that mobility patterns obtained from Twitter data are amenable to quantitatively reflect the mobility dynamics in COVID-19 pandemic at various geographic scales. Globally, the proposed two distances measured from Twitter had greatly deviated from their baselines after March 11, 2020, when WHO declared COVID-19 as a pandemic. The considerably less periodicity after the declaration suggests that the protection measures have obviously affected people's weekly routines. The global *MRI* reveals less responsiveness in May compared with April. At the country scale, the country-level discrepancies in responsiveness are obvious, evidenced by the contrasting mobility patterns in different epidemic phases. We further find that the triggers of mobility changes correspond well with the announcements of mitigation measures, which in return proves that Twitter-based mobility, to some degree, implies the effectiveness of those measures. At the U.S. state scale, the influence of the COVID-19 pandemic on mobility is distinct, as the drop of mobility in most of the states happened in mid-March following the National Emergency declaration on March 13. However, the impacts varied substantially among states. Heavily hit states generally experienced sharp mobility reduction while states with low numbers of cases exhibited relatively marginal mobility reduction. With orders gradually being lifted since late-April, 45 states (except MT, NH, and WA) have shown reduced responsiveness in May compared to April. The methodological knowledge and contextual findings in this study seed future applications of the easily accessible, less privacy-concerning, highly spatiotemporal Twitter data in monitoring multi-scale mobility dynamics during disaster events.

Supporting information

S1 Fig. Temporal distribution of NMI_{sd} and NMI_{cd} for the other 16 selected countries in February, March, April, and May.
(TIF)

S2 Fig. The user count with the number of tweets posted per day.
(TIF)

S1 Table. Country names and accumulated user count for distance calculation in selected countries.
(DOCX)

S2 Table State abbreviations, state names, and accumulated user count for distance calculation in the CONUS states.
(DOCX)

Author Contributions

Conceptualization: Zhenlong Li, Xiaoming Li, Dwayne Porter.

Data curation: Zhenlong Li.

Formal analysis: Xiao Huang.

Funding acquisition: Zhenlong Li, Xiaoming Li, Dwayne Porter.

Methodology: Xiao Huang, Zhenlong Li, Yuqin Jiang.

Project administration: Zhenlong Li.

Resources: Zhenlong Li.

Supervision: Zhenlong Li.

Visualization: Xiao Huang, Yuqin Jiang.

Writing – original draft: Xiao Huang.

Writing – review & editing: Zhenlong Li, Yuqin Jiang, Xiaoming Li, Dwayne Porter.

References

1. Coronavirus Disease (COVID-19) Situation Reports—155 [Internet]. World Health Organization. World Health Organization; [cited 2020Jun23]. Available from: https://www.who.int/docs/default-source/coronaviruse/situation-reports/20200623-covid-19-sitrep-155.pdf?sfvrsn=ca01ebe_2
2. Coronavirus Disease (COVID-19)—events as they happen [Internet]. World Health Organization. World Health Organization; [cited 2020Jun23]. Available from: https://www.who.int/emergencies/diseases/novel-coronavirus-2019/events-as-they-happen
3. Soucheray S. US COVID-19 cases surge past 82,000, highest total in world [Internet]. CIDRAP. 2020 [cited 2020Jun23]. Available from: https://www.cidrap.umn.edu/news-perspective/2020/03/us-covid-19-cases-surge-past-82000-highest-total-world
4. Gao S, Rao J, Kang Y, Liang Y, Kruse J. Mapping county-level mobility pattern changes in the United States in response to COVID-19. SIGSPATIAL Special. 2020 Jun 3; 12(1):16–26.
5. Kraemer MU, Yang CH, Gutierrez B, Wu CH, Klein B, Pigott DM, et al. The effect of human mobility and control measures on the COVID-19 epidemic in China. Science. 2020 May 1; 368(6490):493–7. https://doi.org/10.1126/science.abb4218 PMID: 32213647
6. Shim E., Tariq A., Choi W., Lee Y., & Chowell G. (2020). Transmission potential and severity of COVID-19 in South Korea. *International Journal of Infectious Diseases*. https://doi.org/10.1016/j.ijid.2020.03.031 PMID: 32198088
7. Qiu J, Shen B, Zhao M, Wang Z, Xie B, Xu Y. A nationwide survey of psychological distress among Chinese people in the COVID-19 epidemic: implications and policy recommendations. General psychiatry. 2020; 33(2). https://doi.org/10.1136/gpsych-2020-100213 PMID: 32215365
8. Maier BF, Brockmann D. Effective containment explains subexponential growth in recent confirmed COVID-19 cases in China. Science. 2020 May 15; 368(6492):742–6. https://doi.org/10.1126/science.abb4557 PMID: 32269067
9. Livingston E, Bucher K. Coronavirus disease 2019 (COVID-19) in Italy. Jama. 2020 Apr 14; 323 (14):1335–. https://doi.org/10.1001/jama.2020.4344 PMID: 32181795
10. Mahase E. Covid-19: UK starts social distancing after new model points to 260 000 potential deaths.
11. Oliver N, Letouzé E, Sterly H, Delataille S, De Nadai M, Lepri B, et al. Mobile phone data and COVID-19: Missing an opportunity?. arXiv preprint arXiv:2003.12347. 2020 Mar 27.
12. Engle S, Stromme J, Zhou A. Staying at home: mobility effects of covid-19. Available at SSRN. 2020 Apr 2.
13. Buckee CO, Balsari S, Chan J, Crosas M, Dominici F, Gasser U, et al. Aggregated mobility data could help fight COVID-19. Science (New York, NY). 2020 Apr 10; 368(6487):145. https://doi.org/10.1126/science.abb8021 PMID: 32205458
14. O'reilly T. What is Web 2.0: Design patterns and business models for the next generation of software. Communications & strategies. 2007 Mar 1(1):17.

15. McAfee A, Brynjolfsson E, Davenport TH, Patil DJ, Barton D. Big data: the management revolution. Harvard business review. 2012 Oct 1; 90(10):60–8. PMID: 23074865

16. Goodchild MF. Citizens as sensors: the world of volunteered geography. GeoJournal. 2007 Aug 1; 69 (4):211–21.

17. Scott M, Cerulus L, Kayali L. European Commission tells carriers to hand over mobile data in coronavirus fight [Internet]. POLITICO. [cited 2020Jun24]. Available from: https://www.politico.com/news/2020/03/24/europe-mobile-data-coronavirus-146074

18. Bengtsson L, Gaudart J, Lu X, Moore S, Wetter E, Sallah K, et al. Using mobile phone data to predict the spatial spread of cholera. Scientific reports. 2015 Mar 9; 5:8923. https://doi.org/10.1038/srep08923 PMID: 25747871

19. Wesolowski A, Qureshi T, Boni MF, Sundsøy PR, Johansson MA, Rasheed SB, et al. Impact of human mobility on the emergence of dengue epidemics in Pakistan. Proceedings of the National Academy of Sciences. 2015 Sep 22; 112(38):11887–92. https://doi.org/10.1073/pnas.1504964112 PMID: 26351662

20. Wesolowski A, Eagle N, Tatem AJ, Smith DL, Noor AM, Snow RW, et al. Quantifying the impact of human mobility on malaria. Science. 2012 Oct 12; 338(6104):267–70.

21. Pepe E, Bajardi P, Gauvin L, Privitera F, Lake B, Cattuto C, et al. COVID-19 outbreak response: a first assessment of mobility changes in Italy following national lockdown. medRxiv. 2020 Jan 1.

22. Lyons K. Governments around the world are increasingly using location data to manage the coronavirus [Internet]. The Verge. The Verge; 2020 [cited 2020Jun24]. Available from: https://www.theverge.com/2020/3/23/21190700/eu-mobile-carriers-customer-data-coronavirus-south-korea-taiwan-privacy

23. Giglio M. Would You Sacrifice Your Privacy to Get Out of Quarantine? [Internet]. The Atlantic. Atlantic Media Company; 2020 [cited 2020Jun24]. Available from: https://www.theatlantic.com/politics/archive/2020/04/coronavirus-pandemic-privacy-civil-liberties-911/609172/

24. Park S, Choi GJ, Ko H. Information technology–based tracing strategy in response to COVID-19 in South Korea—privacy controversies. Jama. 2020 Apr 23.

25. Hasan S, Zhan X, Ukkusuri SV. Understanding urban human activity and mobility patterns using large-scale location-based data from online social media. InProceedings of the 2nd ACM SIGKDD international workshop on urban computing 2013 Aug 11 (pp. 1–8).

26. Raman A. How do social media, mobility, analytics and cloud computing impact nonprofit organizations? A pluralistic study of information and communication technologies in Indian context. Information Technology for Development. 2016 Jul 2; 22(3):400–21.

27. Jiang Y, Li Z, Cutter SL. Social network, activity space, sentiment, and evacuation: what can social media tell us?. Annals of the American Association of Geographers. 2019 Nov 2; 109(6):1795–810.

28. Huang X, Li Z, Wang C, Ning H. Identifying disaster related social media for rapid response: a visual-textual fused CNN architecture. International Journal of Digital Earth. 2019 Jun 25:1–23.

29. Huang X, Wang C, Li Z. Reconstructing flood inundation probability by enhancing near real-time imagery with real-time gauges and tweets. IEEE Transactions on Geoscience and Remote Sensing. 2018 May 28; 56(8):4691–701.

30. Martín Y, Cutter SL, Li Z, Emrich CT, Mitchell JT. Using geotagged tweets to track population movements to and from Puerto Rico after Hurricane Maria. Population and Environment. 2020 Feb 3:1–24.

31. Zou L, Lam NS, Shams S, Cai H, Meyer MA, Yang S, et al. Social and geographical disparities in Twitter use during Hurricane Harvey. International Journal of Digital Earth. 2019 Nov 2; 12(11):1300–18.

32. Martín Y, Li Z, Cutter SL. Leveraging Twitter to gauge evacuation compliance: Spatiotemporal analysis of Hurricane Matthew. PLoS one. 2017 Jul 28; 12(7):e0181701. https://doi.org/10.1371/journal.pone.0181701 PMID: 28753667

33. Du E, Cai X, Sun Z, Minsker B. Exploring the role of social media and individual behaviors in flood evacuation processes: An agent-based modeling approach. Water Resources Research. 2017 Nov 1; 53 (11):9164–80.

34. Beiró MG, Panisson A, Tizzoni M, Cattuto C. Predicting human mobility through the assimilation of social media traces into mobility models. EPJ Data Science. 2016 Dec 1; 5(1):30.

35. Hu L, Li Z, Ye X. Delineating and modeling activity space using geotagged social media data. Cartography and Geographic Information Science. 2020 May 3; 47(3):277–88.

36. Liu X, Huang Q, Gao S. Exploring the uncertainty of activity zone detection using digital footprints with multi-scaled DBSCAN. International Journal of Geographical Information Science. 2019 Jun 3; 33 (6):1196–223.

37. Lenormand M, Tugores A, Colet P, Ramasco JJ. Tweets on the road. PloS one. 2014 Aug 20; 9(8): e105407. https://doi.org/10.1371/journal.pone.0105407 PMID: 25141161

38. Dredze M. How social media will change public health. IEEE Intelligent Systems. 2012 Aug 24; 27 (4):81–4.

39. Kass-Hout TA, Alhinnawi H. Social media in public health. Br Med Bull. 2013 Oct; 108(1):5–24.

40. Martín Y, Cutter SL, Li Z. Bridging twitter and survey data for evacuation assessment of Hurricane Matthew and Hurricane Irma. Natural hazards review. 2020 May 1; 21(2):04020003.

41. Warren MS, Skillman SW. Mobility changes in response to COVID-19. arXiv preprint arXiv:2003.14228. 2020 Mar 31.

42. Leguay J, Friedman T, Conan V. Evaluating mobility pattern space routing for DTNs. arXiv preprint cs/0511102. 2005 Nov 29.

43. Roberts S, Osborne M, Ebden M, Reece S, Gibson N, Aigrain S. Gaussian processes for time-series modelling. Philosophical Transactions of the Royal Society A: Mathematical, Physical and Engineering Sciences. 2013 Feb 13; 371(1984):20110550.

44. Pollnow S, Pilia N, Schwaderlapp G, Loewe A, Dössel O, Lenis G. An adaptive spatio-temporal Gaussian filter for processing cardiac optical mapping data. Computers in Biology and Medicine. 2018 Nov 1; 102:267–77. https://doi.org/10.1016/j.compbiomed.2018.05.029 PMID: 29891242

45. Chinazzi M, Davis JT, Ajelli M, Gioannini C, Litvinova M, Merler S, et al. The effect of travel restrictions on the spread of the 2019 novel coronavirus (COVID-19) outbreak. Science. 2020 Apr 24; 368 (6489):395–400. https://doi.org/10.1126/science.aba9757 PMID: 32144116

46. Gatto M, Bertuzzo E, Mari L, Miccoli S, Carraro L, Casagrandi R, et al. Spread and dynamics of the COVID-19 epidemic in Italy: Effects of emergency containment measures. Proceedings of the National Academy of Sciences. 2020 May 12; 117(19):10484–91. https://doi.org/10.1073/pnas.2004978117 PMID: 32327608

47. Xu S, Li Y. Beware of the second wave of COVID-19. The Lancet. 2020 Apr 25; 395(10233):1321–2. https://doi.org/10.1016/S0140-6736(20)30845-X PMID: 32277876

48. Kemp S. Digital 2020: April Global Statshot—DataReportal–Global Digital Insights [Internet]. DataReportal. DataReportal–Global Digital Insights; 2020 [cited 2020Jun24]. Available from: https://datareportal.com/reports/digital-2020-april-global-statshot

49. Kuniya T. Prediction of the epidemic peak of coronavirus disease in Japan, 2020. Journal of clinical medicine. 2020 Mar; 9(3):789.

50. Japan to declare nationwide state of emergency as virus spreads [Internet]. The Japan Times. [cited 2020Jun24]. Available from: https://www.japantimes.co.jp/news/2020/04/16/national/state-of-emergency-expansion/

51. Normile D. Japan ends its COVID-19 state of emergency [Internet]. Science. 2020 [cited 2020Jun24]. Available from: https://www.sciencemag.org/news/2020/05/japan-ends-its-covid-19-state-emergency

52. Opening Up America Again [Internet]. The White House. The United States Government; [cited 2020Jun24]. Available from: https://www.whitehouse.gov/openingamerica/

53. Jun SW. Movement control order not a lockdown, says former health minister: Malay Mail [Internet]. Malaysia | Malay Mail. Malay Mail; 2020 [cited 2020Jun24]. Available from: https://www.malaymail.com/news/malaysia/2020/03/17/movement-control-order-not-a-lockdown-says-former-health-minister/1847232

54. Coronavirus Disease (COVID-19) Situation Reports—43 [Internet]. World Health Organization. World Health Organization; [cited 2020Jun23]. Available from: https://www.who.int/docs/default-source/coronaviruse/situation-reports/20200303-sitrep-43-covid-19.pdf?sfvrsn=76e425ed_2

55. Saudi Arabia suspending domestic flights, mass land transport in fight against COVID-19 [Internet]. Arab News. Arabnews; 2020 [cited 2020Jun24]. Available from: https://www.arabnews.com/node/1644101/saudi-arabia

56. Fisher D, Wilder-Smith A. The global community needs to swiftly ramp up the response to contain COVID-19. The Lancet. 2020 Apr 4; 395(10230):1109–10. https://doi.org/10.1016/S0140-6736(20)30679-6 PMID: 32199470

57. Mervosh S, Lu D, Swales V. See Which States and Cities Have Told Residents to Stay at Home [Internet]. The New York Times. The New York Times; 2020 [cited 2020Jun24]. Available from: https://www.nytimes.com/interactive/2020/us/coronavirus-stay-at-home-order.html?auth=login-google

58. Lin Y. 10 Twitter Statistics Every Marketer Should Know in 2020 [Infographic] [Internet]. Oberlo. 2020 [cited 2020Jun24]. Available from: https://www.oberlo.com/blog/twitter-statistics

59. Mislove A, Lehmann S, Ahn YY, Onnela JP, Rosenquist JN. Understanding the demographics of Twitter users. InFifth international AAAI conference on weblogs and social media 2011 Jul 5.

60. Schradie J. The digital production gap: The digital divide and Web 2.0 collide. Poetics. 2011 Apr 1; 39 (2):145–68.

61. Hawelka B, Sitko I, Beinat E, Sobolevsky S, Kazakopoulos P, Ratti C. Geo-located Twitter as proxy for global mobility patterns. Cartography and Geographic Information Science. 2014 May 27; 41(3):260–71. https://doi.org/10.1080/15230406.2014.890072 PMID: 27019645

62. Gonzalez MC, Hidalgo CA, Barabasi AL. Understanding individual human mobility patterns. nature. 2008 Jun; 453(7196):779–82. https://doi.org/10.1038/nature06958 PMID: 18528393

63. Järv O, Ahas R, Witlox F. Understanding monthly variability in human activity spaces: A twelve-month study using mobile phone call detail records. Transportation Research Part C: Emerging Technologies. 2014 Jan 1; 38:122–35.

64. Huang X, Li Z, Jiang Y, Ye X, Deng C, Zhang J, et al. The characteristics of multi-source mobility datasets and how they reveal the luxury nature of social distancing in the US during the COVID-19 pandemic. medRxiv. 2020 Jan 1. https://doi.org/10.1101/2020.07.31.20143016

65. Valkanas G, Katakis I, Gunopulos D, Stefanidis A. Mining twitter data with resource constraints. In2014 IEEE/WIC/ACM International Joint Conferences on Web Intelligence (WI) and Intelligent Agent Technologies (IAT) 2014 Aug 11 (Vol. 1, pp. 157–164). IEEE.